First observation of ortho-positronium with the J-PET tomograph

K. Dulski[1], **S.D. Bass**[1,2], **J. Chhokar**[1], **N. Chug**[1], **C. Curceanu**[3],
E. Czerwiński[1], **M. Dadgar**[1], **J. Gajewski**[4], **A. Gajos**[1], **M. Gorgol**[5],
R. Del Grande[3], **B. C. Hiesmayr**[6], **B. Jasińska**[5], **K. Kacprzak**[1],
Ł. Kapłon[1], **H. Karimi**[1], **D. Kisielewska**[1], **K. Klimaszewski**[7], **P. Kopka**[7],
G. Korcyl[1], **P. Kowalski**[7], **T. Kozik**[1], **N. Krawczyk**[1], **W. Krzemień**[8],
E. Kubicz[1], **P. Małczak**[9], **M. Mohammed**[1,10], **Sz. Niedźwiecki**[1],
M. Pałka[1], **M. Pawlik-Niedźwiecka**[1], **M. Pędziwiatr**[9], **L. Raczyński**[7],
J. Raj[1], **A. Ruciński**[4], **S. Sharma**[1], **Shivani**[1], **R.Y. Shopa**[7], **M. Silarski**[1],
M. Skurzok[1], **E.Ł. Stępień**[1], **F. Tayefi**[1], **W. Wiślicki**[7], **B. Zgardzińska**[5],
P. Moskal[1]

[1]Faculty of Physics, Astronomy and Applied Computer Science, Jagiellonian University,30-348 Cracow, Poland
[2]Kitzbühel Centre for Physics, Kitzbühel, Austria
[3]INFN, Laboratori Nazionali di Frascati, 00044 Frascati, Italy
[4]Institute of Nuclear Physics Polish Academy of Sciences, 31-342 Cracow, Poland
[5]Institute of Physics, Maria Curie-Skłodowska University, 20-031 Lublin, Poland
[6]Faculty of Physics, University of Vienna, 1090 Vienna, Austria
[7]Department of Complex Systems, National Centre for Nuclear Research, 05-400 Otwock-Świerk, Poland
[8]High Energy Physics Division, National Centre for Nuclear Research, 05-400 Otwock-Świerk, Poland
[9]2nd Department of General Surgery, Jagiellonian University Medical College, Cracow, Poland
[10]Department of Physics, College of Education for Pure Sciences, University of Mosul, Mosul, Iraq

Abstract The J-PET tomograph is constructed from plastic scintillator strips arranged axially in concentric cylindrical layers. It enables investigations of positronium decays by measurement of the time, position, polarization and energy deposited by photons in the scintillators, in contrast to studies conducted so far with crystal and semiconductor based detection systems where the key selection of events is based on the measurement of the photons' energies. In this article we show that the J-PET tomography system constructed solely from plastic scintillator detectors is capable of exclusive measurements of the decays of ortho-positronium atoms. We present the first positronium production results and its lifetime distribution measurements. The obtained results prove the capability of the J-PET tomograph for (i) fundamental studies of positronium decays (in particular test of discrete symmetries in purely leptonic systems), (ii) positron annihilation lifetime spectroscopy, as well as (iii) molecular imaging diagnostics and (iv) observation of entanglement.

Keywords ortho-positronium, J-PET, TOT, lifetime

1 Introduction

Precision studies of positronium decays are a sensitive probe of Quantum Electrodynamics, QED, and allow for new tests of fundamental symmetries involving charged leptons. Prime topics for experimental investigation include decay rates, tests of discrete symmetries and the search for possible rare and invisible decays of positronium atoms.

The physics of positronium, an "atom" consisting of an electron and a positron, is described by QED with small radiative corrections from Quantum Chromodynamics and from weak interaction effects in the Standard Model. Positronium comes in two ground states, $^1S_0$ para-positronium, denoted p-Ps, with spin equal to zero and $^3S_1$ ortho-positronium, denoted o-Ps, with spin equal to one. p-Ps is slightly lighter by 0.84 meV due to the interaction between the electron and positron spins and also the existence of virtual annihilation processes. Spin-zero p-Ps has a mean lifetime of 125 picoseconds and spin-one o-Ps has a mean lifetime of 142 nanoseconds in vacuum. Reviews of positronium physics are given in [1, 2].

Studies of positronium decays have important applications also in medicine and biology. Inside biological materials the positronium mean lifetime and formation probability depend on the healthiness of the tissue material, its nanostructure and concentration of bioactive molecules, in effect allowing us to distinguish between healthy and altered tissue. These factors are indicative of the stage of development of metabolic disorders of human tissues. Thus, positronium decay studies can provide new input in medical diagnosis [3–7].

A new tool to investigate these processes is the J-PET detector, Jagiellonian Positron Emission Tomograph, developed in Cracow [8, 9]. The J-PET programme focusses on fundamental studies of positronium decays [10–17], in positron annihilation lifetime spectroscopy (PALS) [26] as well as in medical diagnostics [18–22]. J-PET is a new PET device based on plastic scintillators designed for total body scanning in medicine as well as for biological applications [23–26] and fundamental physics research [27] with detection of positronium via Compton rescattered photons in the detector. Feasibility studies for physics investigations with the J-PET detector can be found in [28, 29]. Here, we present the first o-Ps production results and lifetime distributions. These are the first exclusive observations and identification of o-Ps atom decays performed by means of a detector based solely on plastic scintillators, in contrast with other studies conducted so far with crystal and semiconductor based detection systems.

Measurements of positronium decay rates are consistent with QED theoretical predictions although the present experimental uncertainties $\sim \mathcal{O}(10^{-4})$ are much larger than the theoretical uncertainties on the QED calculations, by a factor of 100 for o-Ps and by 10,000 for p-Ps, calling for increased experimental precision [2, 30].

Precision observables in positronium decays can be used to test discrete symmetries C, CP and CPT with charged leptons. Charge conjugation invariance in this system has been tested up to the level of 10^{-6} [10–12]. The symmetries CP [13, 14] and CPT [15, 16] have been tested up to $\mathcal{O}(10^{-3})$. QED final state effects in o-Ps decays can mimic CP, T and CPT violation at the level of 10^{-9} to 10^{-10} [15, 17]. Possible invisible decays of positronium are also an interesting topic of investigation with the J-PET detector [31]. Mirror matter models of dark matter allow a branching ratio for the invisible decay of o-Ps in vacuum to mirror particles up to about 2×10^{-7}, below the present experimental bound of 5.9×10^{-4} [32].

In Section II we describe the J-PET detector setup. Section III discusses the event selection method and results, with Conclusions given in Section IV.

2 J-PET detector and positronium production method

The J-PET detector (Fig. 1-left) is built from plastic scintillator strips arranged in three concentric cylindrical layers [24] (Fig. 1-right). It is equipped with the dedicated solely digital front-end electronics [33] and trigger-less data acquisition system [34], optimised for detection of photons originating from positronium decay and photons from the nuclei deexcitations in the energy region of 1 MeV. The data are analysed with a dedicated analysis and simulation framework [35, 36]. Photons below MeV energy interact in the plastic scintillators predominantly via the Compton effect. Therefore, the information about the energy of the photons is not available directly, and the whole data selection and analysis chain is based on the determination of the time and position of the photon's interaction and its energy deposition. The time and position resolutions achieved with the J-PET detector are about 160 ps and 2 cm, respectively [24].
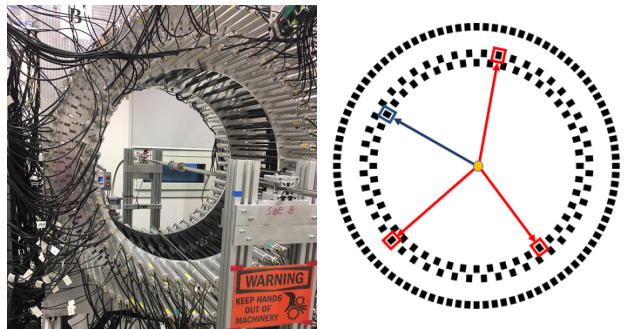

Figure 1 (left) Photograph of the J-PET detector with the annihilation chamber placed in the centre of the detector with a pipe installed on the detector axis. (right) Schematic cross section of the J-PET detector. Black rectangles indicate the cross section of scintillator strips arranged in three concentric cylindrical layers. The arrows indicate annihilation photons (red) from ortho-positronium and the de-excitation photon (blue) emitted by the ^{22}Na source located at the centre of the detector.

Positronium atoms are created from positrons (emitted from the ^{22}Na isotope) and electrons from the porous polymer XAD4 [37]. The polymer was placed inside and annihilation chamber around a ^{22}Na source with activity of 1 MBq, wrapped in a 8 μm thin Kapton foil, as indicated in Fig. 2. The annihilation chamber was installed in the centre of the J-PET detector as can be seen in the photograph in the left panel of Fig. 1. The air was pumped out of the polymer, and during the measurement the pressure in the annihilation chamber was sustained at the level of 10 Pa. The XAD4 polymer was chosen as a positronium production medium since

it is characterized by a high fraction of o-Ps decays into three photons, $f_{3\gamma} = 28.9\%$ [38].

The right panel of Fig. 1 shows an example of an event in which the three photons from o-Ps annihilation, as well as the de-excitation photon from the ^{22}Na source were registered. Exclusive measurements of the interaction's position (and hence relative angles) of the three annihilation photons enable one to reconstruct the full event's kinematics (energies and momenta of all photons) [28]. The additional measurement of the de-excitation photon from the ^{22}Na decay chain (^{22}Na $\rightarrow$ ^{22}Ne* e$^+$ ν $\rightarrow$ ^{22}Ne γ e$^+$ ν) allows one to determine the lifetime of the positronium atom. However, the finite geometrical acceptance and detection efficiency of the J-PET detector, and the multiple Compton scatterings, also mean that there are many other possible event types which need sophisticated selection procedures that we describe in the next section.
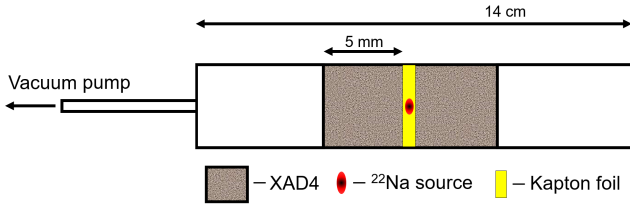

Figure 2 Scheme of the annihilation chamber with the ^{22}Na radioactive source surrounded with XAD4 material. The chamber is connected on one side to the vacuum pump. Chamber details were published in [39].

3 Selection of o-Ps $\rightarrow$ 3γ events

The positron-electron annihilation predominantly leads to the production of two or three photons. It may proceed directly (e$^+$e$^-$ $\rightarrow$ 2γ(3γ)) or via formation of a positronium atom (e$^+$e$^-$ $\rightarrow$ Ps $\rightarrow$ 2γ(3γ)). When requiring registration of the de-excitation photon (needed for the determination of the positron lifetime in the XAD4 material) we may define three classes of events with one (I), two (II) or three (III) registered annihilation photons, as it is graphically depicted in Table 1. In vacuum o-Ps decays only to three photons (due to C symmetry conservation). However, in the intermolecular voids of the material it may decay also into two back-to-back photons via conversion [40] or pick-off [41] processes. The inclusive measurements using categories I, II are typically used both in PALS [38, 40, 42] and in most of the so far conducted experiments aimed at studies of discrete symmetries [11, 13–15].

Table 1 Different types of observed events. Arrows denote registered annihilation photons (red solid), not registered annihilation photons (gray dashed), and deexcitation photon (blue dotted).


Figure 3 Scheme of different kind of events expected in the case of three registered interactions: positronium or direct electron-positron annihilation into 3 photons (left), into two back-to-back photons with additional registration of scattering of one of them (middle), and into 2 photons when one of them is not registered and the other undergoes double scattering (right). For clarity only few scintillators in one detection layer are shown.

Here we concentrated on the exclusive measurement of three photons from the o-Ps $\rightarrow$ 3γ decay, case III in Table 1. Such exclusive measurements enable one to reconstruct the full event kinematics, making all photons' four-momentum vectors available for the physics analysis, suppressing the physical and instrumental background. Measurement of the de-excitation photon allows one to determine the lifetime of the positron in the target, and hence to disentangle between the o-Ps decays from the direct annihilation events (e$^+$e$^-$ $\rightarrow$ 3γ), and to suppress the background originating from p-Ps $\rightarrow$ 2γ decays followed by the secondary scattering of photons in the detector. The latter background is illustrated in the middle and right panels of Fig. 3. De-excitation and annihilation photons are identified based on the measured time-over-threshold (TOT) val-

ues [43] that are correlated with the energy deposition in the scintillators.

Fig. 4 shows a pictorial definition of the TOT values measured with the J-PET front-end electronics [33] (upper panel) and an example TOT spectrum with superimposed regions used for the identification of the de-excitation and annihilation photons (lower panel). Next, the first level of background reduction from rescattering (middle and right panel of Fig. 3), from accidental coincidences and from cosmic rays, was applied as a condition for the distance between the decay plane and the annihilation position, as well as the time difference between the interaction of the annihilation photons' candidates (Δt_{a13}). Due to momentum conservation, momentum vectors of the photons from the o-Ps $\rightarrow 3\gamma$ decay form a plane, subsequently referred to as the decay plane. In the ideal case the decay plane constructed from the measured interaction points should comprise the annihilation point. Therefore, for the o-Ps $\rightarrow 3\gamma$ events, the distance between the decay plane and the
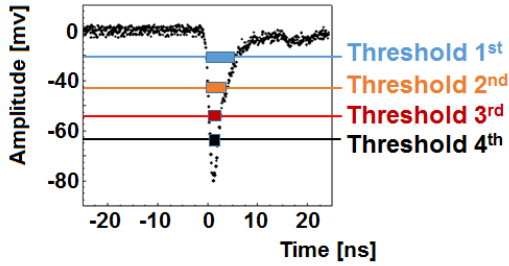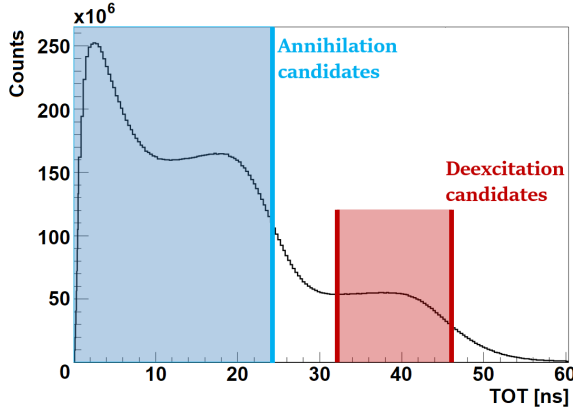

Figure 4 (Upper panel) Pictorial definition of the Time-Over-Threshold (TOT) of the signal measured in the J-PET detector. TOT is a sum of signal widths in the time domain, over four preset voltage levels. (Lower panel) Distribution of the TOT values measured by means of the J-PET detector. Categorization of the Hit is based on the TOT value. In the analysis, the annihilation candidate is defined when TOT value is less than 24 ns. De-excitation candidates corresponds to the TOT greater than 32 ns and smaller than 46 ns.
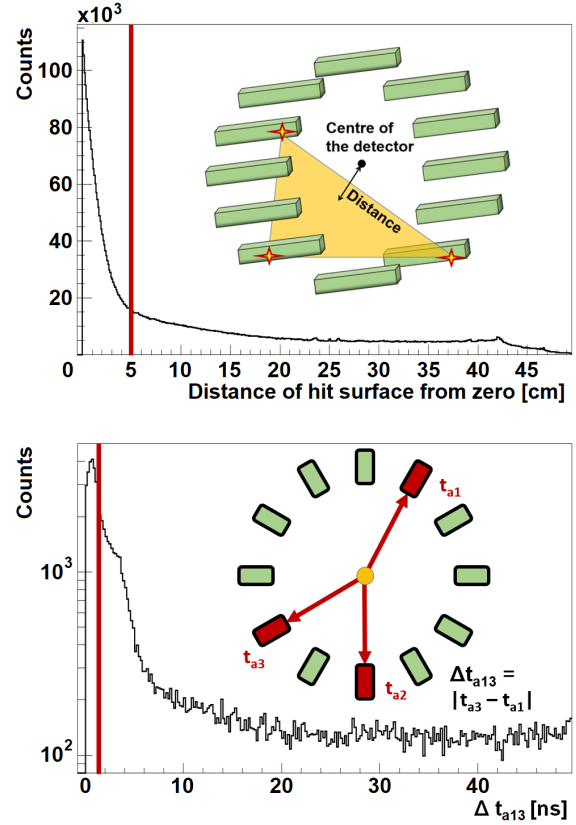

Figure 5 Distributions of the distance of the decay plane from the center of the detector (upper panel), and the time difference Δt_{a13} between annihilation hits (lower panel). Red line indicates the condition which is used for suppressing the background.

centre of the annihilation chamber should be close to zero, while this distance for the background events may spread even up to the radius of the detector, as shown in the upper panel of Fig. 5. Similarly, the reconstructed value of Δt_{a13} should be close to zero in the case of the true o-Ps $\rightarrow 3\gamma$ process, where $\Delta t_{a13} = |t_{a3} - t_{a1}|$ with t_{a3} - the biggest time of registration, and t_{a1} - the smallest time, out of the three determined emission times of the annihilation photons candidates. In the case of the double scattering (right panel of Fig. 3) Δt_{a13} may reach a value of about 6 ns and for accidental coincidences it forms a continuous flat distribution as can be seen in the lower panel of Fig. 5.

Further, as the next stage of the background reduction and identification of the o-Ps $\rightarrow 3\gamma$ events, the angular correlation presented in Fig. 6 is applied. The most pronounced single-scattered background events (middle panel of Fig. 3) form a band at 180 degrees, while the double-scattered background events (right panel of Fig. 3) are concentrated predominantly at the left side of this band. For the true o-Ps $\rightarrow 3\gamma$ decays, due to the momentum conservation, the sum of the two smallest relative angles defined in Fig. 3 is larger than 180
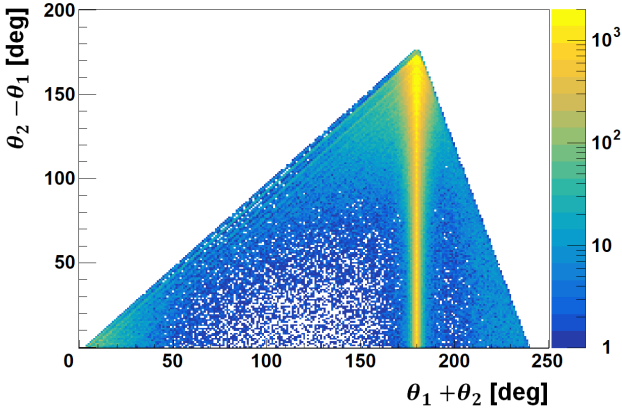
Figure 6 Distribution of the difference versus sum of the two smallest relative angles for three annihilation photon candidates. The most pronounced vertical band at 180 degrees corresponds to events with annihilations into two back-to-back photons with additional scattering of one of them (middle panel of Fig.3). Events on the left side of this band corresponds predominantly to the double scattering (right panel of Fig.3) and the signal from o-Ps $\rightarrow 3\gamma$ process is visible as an enhancement at about 240 degrees.
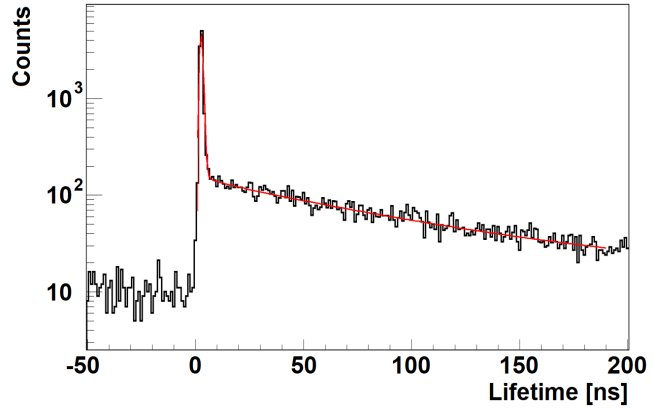

Figure 7 Positron lifetime distribution determined for events with the sum of the two smallest relative angles between the photons larger than 190 degrees. The lifetime was calculated as the difference between the mean time of the emission of annihilation photons and the time of the emission of the de-excitation photon. Red line indicates fit to the data.

degrees and the distribution has the maximum for the symmetric configuration with the sum of relative angles equal to 240 degrees [10, 28]. In Fig. 6 which shows experimental data obtained with the J-PET detector, such enhancement is clearly visible as expected. In order to suppress the background originating from the back-to-back photons, it is required that the sum of two smallest angles is larger than 190 degrees. Further, as the last stage of the selection, a lifetime histogram is used.

Fig. 7 presents our main result, the lifetime spectrum for 3γ events candidates with the sum of the two smallest relative angle larger than 190 degrees. The signal from o-Ps $\rightarrow 3\gamma$ process is seen as a clear exponential decay with the mean lifetime of 90.4 ± 2.9 ns consistent with the value of 90.8 ± 1.2 ns expected for the mean lifetime of ortho-positronium in the used XAD4 porous polymer [38]. This spectrum enables one to reject the background from direct $e^+e^- \rightarrow 3\gamma$ annihilation, for which the lifetime is equal to about 0.5 ns [38]. Also the remaining background from the cosmic radiation and the scatterings in the annihilation chamber concentrates within few nanoseconds around zero (the maximum time needed for cosmic ray to pass through the detector). The flat distribution below the o-Ps lifetime spectrum for the negative lifetime values corresponds to the background events due to the accidental coincidences [34]. This feature enables one to estimate statistically the contribution from the accidental coincidences to the distributions which will be used for the physics studies (such as e.g. Dalitz plot distribution of the o-Ps $\rightarrow 3\gamma$ process).

4 Conclusions

In this article we have shown that the J-PET tomography system constructed solely from plastic scintillator detectors is capable of exclusive measurements of the decays of ortho-positronium atoms. The elaborated selection method is based on the measurement of the time, position and energy deposition of photons in the scintillator strips, in contrast to studies conducted so far with the crystal and semiconductor based detection systems where the key selection of events is based on the measurement of the photons' energies [10–17]. The presented results, such as shown in Fig. 7, show that J-PET detector provides a new tool for fundamental physics studies of positronium decays [2, 27], for positron annihilation lifetime spectroscopy, and for entanglement studies [6, 7]. It also opens new perspectives for investigating the use of positronium as a diagnostic biomarker for medicine [3–5, 18].

References

1. D. B. Cassidy, Eur. Phys. J. D **72** (2018) 53.
2. S. D. Bass, Acta Phys. Polon. B **50** (2019) 1319.
3. P. Moskal, B. Jasińska, E.Ł. Stępień and S.D. Bass, Nat. Rev. Phys. **1** (2019) 527.
4. P. Moskal *et al.*, Phys. Med. Biol. **64** 5 (2019) 055017.
5. P. Moskal *et al.*, `arXiv:1911.06841 [physics.ins-det]`.
6. B.C. Hiesmayr, P. Moskal, Sci. Rep. **7** (2017) 15349.
7. B.C. Hiesmayr, P. Moskal, Sci. Rep. **9** (2019) 8166.
8. P. Moskal *et al.*, Nucl. Instrum. Meth. A **764** (2014) 317.
9. P. Moskal *et al.*, Nucl. Instrum. Meth. A **775** (2015) 54.
10. A. P. Mills and S. Berko, Phys. Rev. Lett. **18** (1967) 420.
11. J. Yang *et al.*, Phys. Rev. A **54** (1996) 1952.
12. P. A. Vetter and S. J. Freedman, Phys. Rev. A **66** (2002) 052505.
13. T. Yamazaki, T. Namba, S. Asai and T. Kobayashi, Phys. Rev. Lett. **104** (2010) 083401; Erratum: [Phys. Rev. Lett. **120** (2018) 239902].
14. M. Skalsey and J. Van House, Phys. Rev. Lett. **67** (1991) 1993.
15. B.K. Arbic et al., Phys. Rev. **A 37** (1988) 3189.
16. P. A. Vetter and S. J. Freedman, Phys. Rev. Lett. **91** (2003) 263401.
17. W. Bernreuther, U. Low, J. P. Ma and O. Nachtmann, Z. Phys. C **41** (1988) 143.
18. P. Moskal, E.Ł. Stępień *Prospects and clinical perspectives of total-body PET imaging using plastic scintillators,* PET Clinics 2020 (in press).
19. S. Vandenberghe, P. Moskal, J. Karp, *State of the art in total body PET*, EJNMMI Physics (2020) (in press), `https://doi.org/10.1186/s40658-020-00290-2`
20. P. J. Slomka, T. Pan and G. Germano, Semin. Nucl. Med., vol. **46** (2016) 5.
21. R.D. Badawi *et al.*, J. Nucl. Med. **60**(3) (2019) 299.
22. J.S. Karp *et al.*, J. Nucl. Med. **61**(1) (2020) 136.
23. P. Moskal *et al.*, Phys. Med. Biol. **61** (2016) 2025.
24. Sz. Niedźwiecki *et al.*, Acta Phys. Polon. B **48** (2017) 1567.
25. P. Kowalski *et al.*, Phys. Med. Biol. **63** (2018) 165008.
26. P. Moskal *et al.*, Phys. Med. Biol. **64** (2019) 055017.
27. P. Moskal *et al.*, Acta Phys. Polon. B **47** (2016) 509.
28. D. Kamińska *et al.*, Eur. Phys. J. C **76** (2016) 445.
29. P. Moskal *et al.*, Eur. Phys. J. C **78** (2018) 970.
30. G. S. Adkins, R. N. Fell and J. Sapirstein, Ann. Phys. **295** (2002) 136.
31. W. Krzemień, E. Pérez del Río, K. Kacprzak Acta Phys. Pol. B **51** (2020) 165.
32. C. Vigo, L. Gerchow, L. Liszkay, A. Rubbia and P. Crivelli, Phys. Rev. D **97** (2018) 092008.
33. M. Pałka *et al.*, JINST **12** (2017) P08001.
34. G. Korcyl *et al.*, IEEE Transactions On Medical Imaging **37** (2018) 2526.
35. W. Krzemień *et al.*, Acta Phys. Polon. B **47** (2016) 561.
36. W. Krzemień *et al.*, SoftwareX 11 (2020) 100487.
37. `https://www.sigmaaldrich.com`, CAS Number 37380-42-0.
38. B. Jasińska *et al.*, Acta Phys. Polon. B **47** (2016) 453.
39. M. Gorgol *et al.*, Acta Phys. Pol. B **51**, (2020) 293
40. P.V. Stepanov *et al.*, Phys. Chem. Chem. Phys. **22** (2020) 5123.
41. R.L. Garwin, Phys. Rev. **91** (1953) 1571.
42. Y.C. Jean, P.E. Mallon and D.M. Schrader, *Principles and Applications of Positron and Positronium Chemistry* (World Scientific, 2003) 1.
43. S. Sharma *et al.*, to appear in EJNMMI, `arXiv:1911.12059 [physics.ins-det]`.